Gleb Kleyman*, Tong Kang, Jens Twiefel and Walter Voit

Characterization of Triboelectric Charge Generation between PTFE and Nylon after Repeated Contacts

https://doi.org/10.1515/ehs-2018-0001

Abstract: The charge generation between PTFE and Nylon 6,6 has been analyzed under different settings of temperature, humidity and mechanical load. It is found that the charging characteristics of the sample materials in terms of the parameters investigated in this study (e.g. temperature, relative humidity and applied force) are linear. Furthermore, the experimental results show that the proportionality factor between applied load and maximum achievable surface charge is affected by the sample temperature. As we show this fact is most likely attributed to the strongly temperature-dependent elastic properties of polymeric materials. The discoveries lead us to a mathematical formulation for the surface charge density which allows the investigation of maximum charge density for every single operating point within the parameter variation limits. The model parameter for two different structured material pairs are obtained from measurements and applied to the mathematical formulation. The theoretical data demonstrates that the proportionality factor between sample temperature and surface charge is strongly affected by relative humidity.

Keywords: triboelectric, TENG, electrostatic charging

Tong Kang: Department of Mechanical Engineering, University of Texas at Dallas, Richardson, Texas, USA,

E-mail: tong.kang@utdallas.edu

Jens Twiefel: Institute of Dynamics and Vibration Research, Leibniz Universitat Hannover, Hannover, Germany,

E-mail: twiefel@ids.uni-hannover.de

Walter Voit: Department of Mechanical Engineering, University of Texas at Dallas, Richardson, Texas, USA,

E-mail: walter.voit@utdallas.edu

Introduction – State of the Art

In the past few years triboelectric generators have become a promising technology in mechanical to electrical energy conversion (Wang 2013). Especially for energy harvesting application, the triboelectric effect enables new application scenarios and techniques (Ha et al. 2015). The triboelectric effect describes charge segregation on the surface of two different materials after coming into contact, known also as electrostatic charging. After contact an electrostatic attraction force acts between the oppositely charged materials. Mechanical energy can be converted into electricity when the attracted parts are displaced by mechanical force. This principle is similar to electrostatic generators (Bright and Makin 1969) with the benefit of a self charging character. Nevertheless the triboelectric energy conversion mechanism prompts questions. In particular, scientists are questioning the root of charge separation (Lacks and Sankaran 2011). Additionally there is always a desire to enhance the power output of energy harvesting systems, and for triboelectric systems this can be achieved either by optimizing design features (Tang et al. 2014) or material properties (Chun et al. 2015). There are two basic working modes of triboelectric generators studied, the sliding and the contact mode. In sliding mode the generators are designed for lateral relative motion as rotors of wind or water turbines (Zhu et al. 2014) whereas in contact-separation mode the parts are moved closer and then separated in a linear motion (Niu et al. 2013). The charge density on the two surfaces is an important factor that determines the performance of a triboelectric generator, but today's modeling approaches for triboelectric (nano-)generators consider only constant surface charges and not the charging characteristics of the materials (Niu and Wang 2015). Few publications are dedicated to the charge generation mechanism on the surface between triboelectric material pairs. As stated by Z. L. Wang (Wang 2014): "...the mechanism behind triboelectrification is still being studied...". Therefore it is necessary to broaden the understanding of triboelectric charging such that there may be better designed energy harvesting systems in the future.

^{*}Corresponding author: Gleb Kleyman, Institute of Dynamics and Vibration Research, Leibniz Universitat Hannover, Hannover, Germany, E-mail: kleyman@ids.uni-hannover.de

One of the challenges in triboelectric research is the large number of influential parameters on the surface charge density and the interaction of those parameters, causing many researchers to debate on the exact mechanism. The charge transfer might be caused by thermodynamic, chemical or physical effects (Galembeck et al. 2014). However the contribution of **temperature** and **rel**ative humidity to charge separation has been proved experimentally (Greason 2000). It was also found that another important parameter is the surface roughness, explaining why a current method to maximize the surface charge is micro and nano structuring of materials (Lee et al. 2013). An applied load leads to deformation of a surface and a change of the contact area, therefore another important parameter is the contact force between the materials (Liu, Oxenham, and Seyam 2013). Unlike previous publications we are also considering the Young's modulus as a crucial factor since it defines the relationship between force and deformation. Previous studies of triboelectric charging were limited to the variation of one or two of those parameters at a time and their results are at times contradictory, see Table 3. The relatively large number of parameters makes more exhaustive studies infeasible and is the reason why interactions of parameter variations are often overlooked. In this paper, we are studying the influence of the previously mentioned parameters on surface charge density all at the same time. This holistic approach provides new insights about the triboelectric charging mechanism between PTFE and Nylon, showing previously unknown correlation between surface roughness and the impact of temperature respectively humidity to charge generation. However this theory is based on an interpolation of our measurements and thus should be assumed under reservation. Still this hypothesis gives new impulses for the triboelectric research. Compared to different studies in Table 3 it is evident that we were able to gather useful data and broaden the knowledge of charge generation on the PTFE/Nylon interface layer. For future researchers this will enable the development of a holistic modeling approach for triboelectric energy harvesting systems including mechanical, electrical and material properties. Specifically, this will help in:

- developing materials with optimized properties
- designing of more efficient triboelectric energy harvesting devices embedded into given mechanical structures
- optimizing the geometry and electrical properties for quasi-static or resonant working regimes

Theory and Model of Triboelectric **Energy Generators**

For a general understanding of the triboelectric energy harvesting mechanism we are breaking down the complex system into a triboelectric and an electrostatic subsystem. These two subsystems are assigned to different roles, namely charging and energy converting. In current applications the standalone triboelectric effect does not generate any utilizable electric energy - only the electrostatic effect completes the system successfully and makes it a working energy converter. Therefore it must be said that the terminology triboelectric energy harvesting is misleading and aggravates the vision of the mechanism for third parties.

For illustrative purposes the triboelectric energy conversion can be compared to a hydrostatic analogue as shown in Figure 2: Let's assume a rubber balloon is connected to a vertical pipe where inside the pipe there is a turbine which is able to convert a fluid stream into electricity. Now the balloon is getting filled with a defined volume of fluid (here: fluid ≜ charge) and the fluid streams though the pipe until a steady state condition between the hydrostatic head and the pressure of the balloon walls is reached. Energy can only be extracted from the turbines rotation as long as it gets propelled by the fluid stream. An alternating volume change of the balloon affects the hydrostatic head rising and falling which drives the turbine inside the pipe (volume change ≜ electrostatic effect). In this analogy the triboelectric charge defines the volume of fluid and the electrostatic effect the volume change. We can state that the triboelectric effect is an essential precondition for the energy conversion, however the electrostatic effect is the real driving mechanism of an electrical AC-current. Figure 1 shows the triboelectric/electrostatic dual-system as a black box model resulting from this theoretical formulation. The output variable is the electrical power and the input variables are the mechanical excitation together with material properties. Within the system's boundaries there is the triboelectric charging mechanism and the electrostatic effect and thus the efficiency of the entire system is closely tied to both the surface charge density and the capability of the electrostatic system to convert energy. The two critical factors for a high power output triboelectric generator are a well designed electrostatic energy converter and a maximized surface charge density.

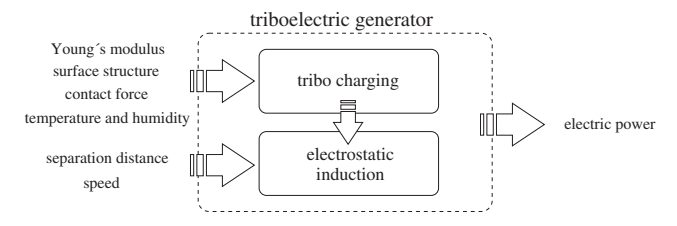


Figure 1: Black box model of the triboelectric generator.

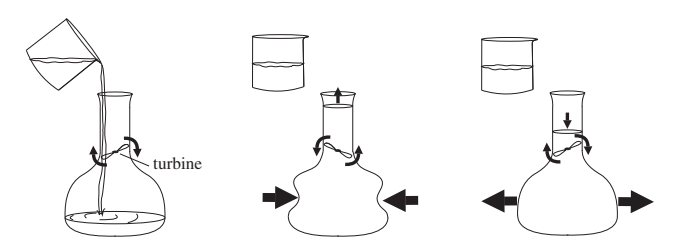


Figure 2: Analogy of the triboelectric energy harvesting mechanism.

Electrostatic Energy Conversion

The goal of this section is to show that the surface charge is the crucial factor in triboelectric energy conversion. Therefor it is looked at the electrostatic subsystem first. An electrostatic energy converter for linear motion can be simplified as a series connection of capacitors as shown in Figure 3. The air gap capacitance C(x) is variable while $C_{\rm PTFE}$ and $C_{\rm Nylon}$ are given by the converters geometry and material properties. The surface charge is assigned to Q_n (surface charge density multiplied by contact area) and the electric load is assigned to Z. Once the air gap x increases the variable capacitance C(x) decreases:

$$C(x) = \varepsilon_0 \frac{A}{x} \tag{1}$$

Here ε_0 is the dielectric constant in air and A the cross section area of the converter. Since the surface charge Q_n is constant (between contacts) there is a rising voltage V(x) across the air gap capacitance according to

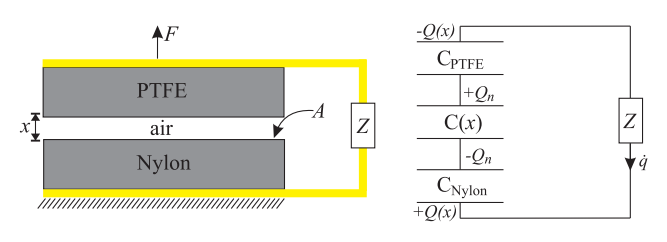


Figure 3: Electrostatic Energy Converter for linear motion.

$$V(x) = \frac{Q_n}{C(x)}. (2)$$

Corresponding to Kirchhoff's circuit laws the directed sum of all voltages around the closed network in Figure 3) is equal to zero. Therefore the rising voltage V(x) affects a charge flow \dot{q} inside the circuit. As a result the charge Q(x) is transferred from the backside electrode of one material to another (here PTFE and Nylon).

There is always an electrostatic attractive force acting between two oppositely charged objects. The electric field E is assumed to be homogeneous for small displacements (compared to the object's surface area). Thus a linear equation describes the attractive force as

$$F_{\text{att}} = O_n E. \tag{3}$$

After applying eq. (1)–(2) and the definition of a homogeneous electric field $(E = \frac{V}{x})$ on eq. (3), the definition of the electrostatic force acting at an triboelectric contact mode energy converter results in

$$F_{\text{att}} = \frac{Q_n^2}{\varepsilon_0 A}.$$
 (4)

Equation 4 shows that the attraction force is only dependent on the surface charge and not on the separation distance. The total amount of converted energy depends strongly on the mechanical force brought into the system to compensate for this attraction. A higher surface charge increases energy conversion. For a charge constrained cycle (which is the case here between contacts) the converted energy can be expressed as (Boisseau, Despesse, and Seddik 2012)

$$E_{\rm conv} = \frac{1}{2}Q_n^2 \left(\frac{1}{C_{\rm min}} - \frac{1}{C_{\rm max}}\right). \tag{5}$$

Assuming that the displacement x_{min} during contact is nearly zero and applying eq. (1) the expression can be simplified to

$$E_{\rm conv} = \frac{1}{2} Q_n^2 \left(\frac{1}{C_{\rm min}} \right) = \frac{1}{2} Q_n^2 \left(\frac{x_{\rm max}}{\varepsilon_0 A} \right). \tag{6}$$

As eq. (6) shows the amount of converted energy grows with the maximum displacement x_{max} and is even quadratic to the surface charge. In terms of a real life energy harvesting application, a high power output is desired. A maximum output power can only be reached when the load impedance Z matches the internal impedance of the converter. Here the internal impedance is a series connection of three capacitors. In the case of a sinusoidal displacement x, the optimum load impedance is the

conjugate complex value of the internal impedance:

$$Z_{\rm opt} = \frac{j\omega}{C_{\rm avg}} \tag{7}$$

Here ω is the angular frequency of the displacement and C_{avg} is the average capacitance over a cycle. The electric output power *P* is then given as

$$P = \frac{\partial E}{\partial t} = \frac{1}{2} Q_n^2 \left(\frac{\dot{x}}{\varepsilon_0 A} \right). \tag{8}$$

Equations (6) and (8) prove energy generation and power output grow significantly when the surface charge is enhanced. It can also be seen that the output power for the quasi static consideration is dependent on the moving velocity \dot{x} , however an energy harvesting device is usually mounted to a dynamic mechanical structure. When this is the case the mechanical parameters of the energy harvester system (mass of plates, stiffness and damping of the mounting) can be fit into eq. (8) (Roundy, Wright, and Rabaey 2004). This allows one to estimate the performance of the electrostatic converter under dynamic conditions as well. It results therefrom that the highest power output is achieved when the excitation frequency exactly matches the resonance frequency of the system (Kim, Tadesse, and Priva 2009). This is valid for a linear non-impact type triboelectric device assuming that contact of the materials between the cycles can be ignored. But when the excitation force is high enough and therefore the velocity of the moving plate right before the contact is not equal to zero the mathematical formulation of the system becomes more complex. For this non-linear case there is no solution given here, but methods and techniques for characterization of nonlinear systems can be found in different literature e.g. (Meirovitch 1970).

Triboelectric Charging

Scientist have dealt with the triboelectric charging phenomena for at least 100 years (Shaw 1917). There have been efforts to bring materials in ascending order in terms of the direction of charge transfer as far back as the eighteenth century. Arising from these experiments, the triboelectric series according to Figure 4 has been put forward. Still the mechanisms behind triboelectric charging of insulators is not understood exactly, whereas the contact charging of metals seems to be understood quite well¹.

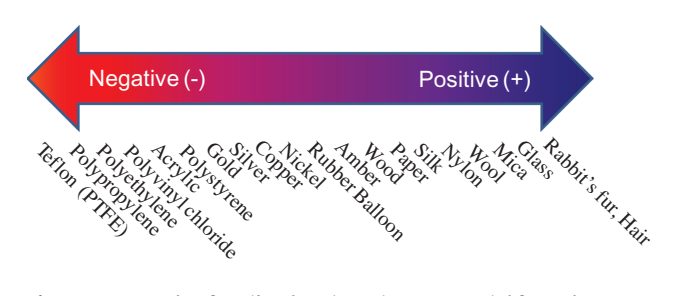


Figure 4: Example of a triboelectric series. A material from the positive side contacted with a material from the negative side will charge positively. Adapted from Lacks and Sankaran (2011).

For insulating materials there exist different theories, an objective overview of the most common theories for triboelectric charging can be found in review papers e.g. (Lacks and Sankaran 2011). However, the physical phenomenon that is causing charge transfer between materials shall not be the subject of the present investigation. Although all of the theories can explain charge separation, none of them can give a quantitative estimation of surface charge depending on parameters such as humidity, temperature, contact force and roughness. Experiments show that these parameters definitely affect triboelectric charging.

It is observed that the surface charge density of triboelectric materials reaches a saturation level after several contacts (Greason 2000). Water and temperature are attributed to have a key role in surface charge saturation levels since they increase conductivity and therewith the surface charge leakage. However, it is debated how strong of an impact these two parameters have on triboelectric charging (Liu, Oxenham, and Seyam 2013). On the other hand surface roughness and contact force are said to increase the magnitude of surface charge when they are increased. The explanation for this lies in the material transfer theory and the mechanochemical theory of triboelectric charging. These theories refer to a transfer of material patches and particles between the different materials caused by stress. The stress increases either with a higher compressive load between the contact partners or with the surface roughness. Knowing this, it is interesting to find out how different combinations of temperature and compression load affect the surface charge as it is known that polymeric materials change their mechanical properties with temperature. Therefore we are investigating the surface charge of a selected material combination depending on temperature, humidity, Young's modulus and roughness. The goal is to give a mathematical description that decrypts the interaction of all those parameters.

¹ work function theory (Greason 2000).

Materials and Methods

In our everyday lives we are surrounded by several synthetic polymers. This is especially true because scientist have learned to systematically control a polymer's behavior in terms of its chemical and physical nature (Peacock and Andrew 2006). Concerning triboelectric energy harvesting, this is an interesting aspect since materials can be designed in order to produce maximum triboelectric charge, which is important for the performance of a triboelectric energy harvesting device as shown in Section 2. In this study we choose Polytetrafluoroethylene (PTFE) and Nylon for the experiments. As Figure 4 shows, the materials are classified far on the opposite sides of the triboelectric series and thus the triboelectric charging between the materials is expected to be very high.

Characterization of the Materials

The materials were obtained from McMaster-Carr as raw sheets in two different thicknesses. The samples were laser-cut into circles of 30 mm diameter. A layer of Ni and Au was deposited by PVD on one side of the samples as shown in Figure 5. Usually PTFE has a slippery and non sticking surface, which is why single sided adhesiveready PTFE sheets were used here. Depending on the

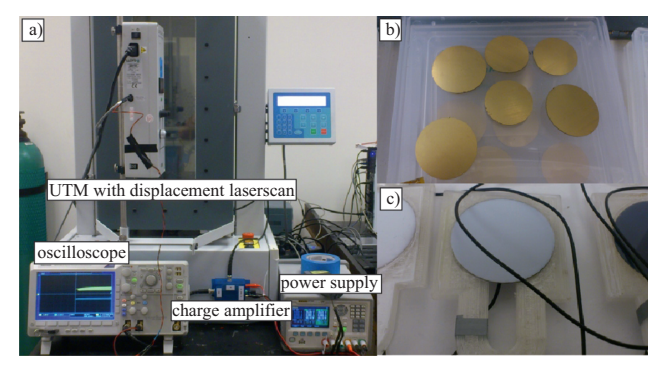


Figure 5: (a) Experimental set up, (b) metalized backside of the samples, (c) front side of PTFE sample (attached to a slider).

Table 1: Sample characteristics.

		Nylon	PTFE	
	No. 1	No. 2	No. 1	No. 2
R _a [μm]	0.06	0.12	0.67	8.49
thickness [mm]	1.62	2.36	1.59	2.42
diameter [mm]	30	30	30	30
temperature and rel. humidity [°C and %]	9/60	25/50	45/17	
series capacitance (PTFE/Nylon) No. 1 [pF]	4.8	5.4	6	
series capacitance (PTFE/Nylon) No. 2 [pF]	4.6	4.9	5.5	

materials thickness, the samples show a different surface topography. As a first step the surface roughness of the samples was characterized and the arithmetic average R_a of surface roughness was calculated; see Table 1. For the experiments, two different thicknesses of each of the two materials were used. Only the corresponding thicknesses were contacted (thin-thin and thick-thick). The topography was characterized with a contact profilometer (stylus radius of 12.5 µm). Figure 6 shows the results of the profilomentry measurements along one direction over a distance of 5 mm. From this measurements the resulting amplitude parameter R_a was calculated. R_a is a common parameter to describe the variations in the height of the surface relative to a reference plane (Bhushan 2000). However different structured materials can have the same R_a values so this is not sufficient for a complete characterization of a surface. That is why the amplitude probability distribution and the Fourier transform of the measurements are also given in Figure 6. From these graphs the variance in surface roughness can be analyzed, which shows that the surface of the Nylon samples is more randomly structured while PTFE is systematically structured. The exact capacitance of PTFE and Nylon is essential for the calculation of the surface charge in the following section. The series capacitance of the samples was measured under light compression for different temperature settings with a HP 4192A LF impedance analyzer. Over a range of temperatures, polymers show a massive change in their physical properties which is known as the glasstransition. Glass-transition denotes the reversible change in stiffness of amorphous materials from a hard and brittle state into a soft state, therefore a temperature change will affect the deformation on the surface of materials under compression. A possible consequence is a change of real contact area and therewith a change in triboelectric charging characteristics. From literature it is known that Nylon and PTFE have a significant drop of the Young's modulus curve somewhere in a temperature range between 20°C and 60°C (Calleja et al. 2013; Rae 2004; Evstatiev 1997).

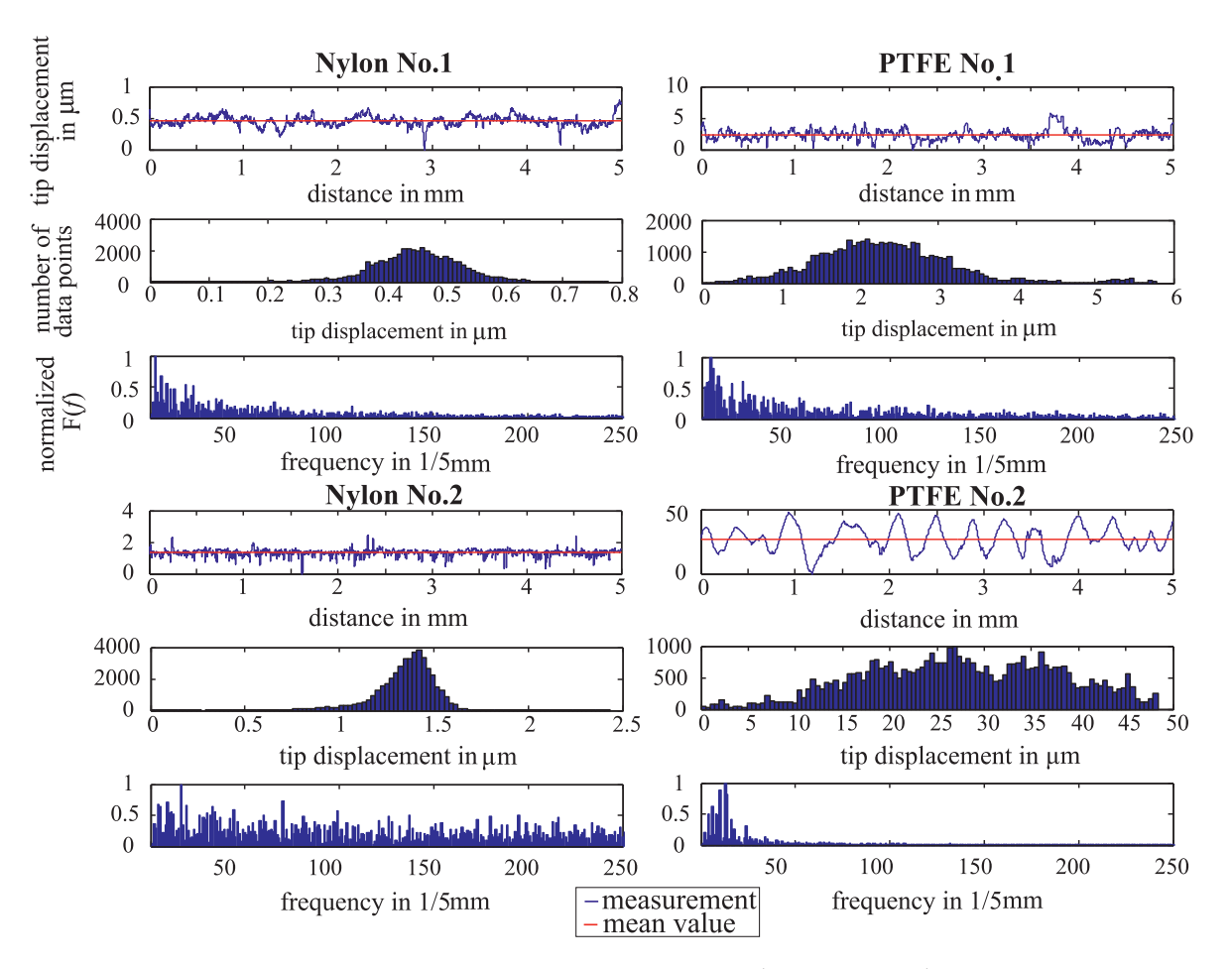


Figure 6: Surface topography of samples. Measured with a contact profilometer (12.5 µm tip radius). Top: stylus displacement over a 5 mm measuring distance. Middle: amplitude probability distribution. Bottom: Fourier transform of surface roughness measurement.

Therefore a dynamic mechanical analysis (DMA) was performed on the sample materials. The result is shown in Figure 7. At the three specific temperature settings the storage modulus E' is highlighted by dotted lines.

Experimental Setup

The samples were compressed and separated on a universal testing machine (UTM) by Lloyd Instruments, which provides a force measurement up to 500 N in the direction of movement and has a laser displacement sensor. Additionally the machine is equipped with a controllable temperature chamber as Figure 5 shows. The chamber can be heated up by thermoelectric elements and cooled down by liquid nitrogen inflow. All samples were bonded to 3-D printed slides that fit onto two compression plates. The lateral movement of the compression plates is avoided as they were guided by three metal rods. The relative displacement of the plates and the charge transfer between the sample electrodes were tracked simultaneously with an oscilloscope from which the surface charge was later calculated.

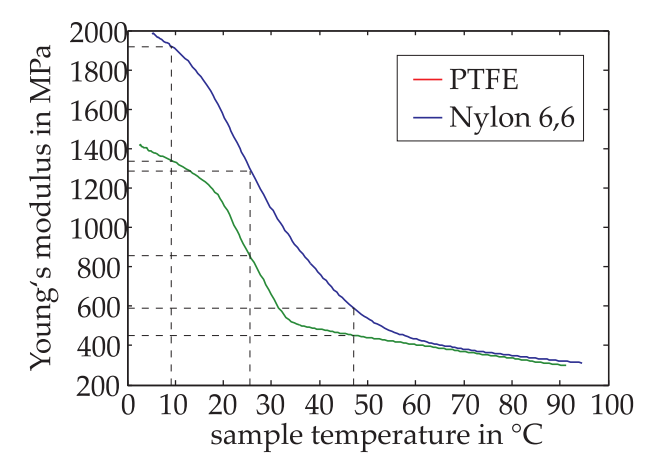


Figure 7: Storage modulus E' from a low-constant-frequency temperature-sweep DMA.

The surface charge measurement was implemented by connecting a charge amplifier to the circuit instead of an electric load according to Figure 8. A charge amplifier acts as a current integrator and produces a voltage output U_a proportional to the integrated value of the input current \dot{q} .

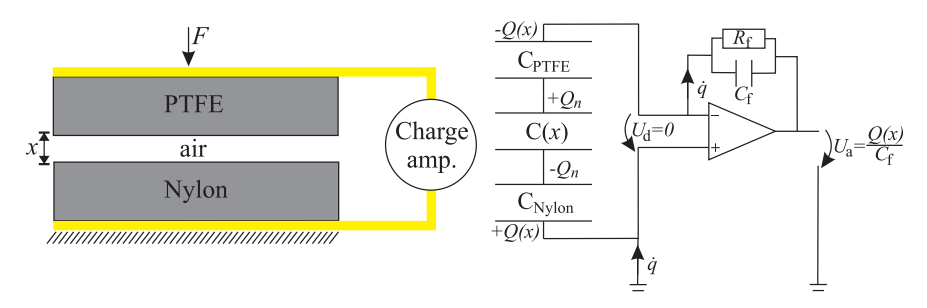


Figure 8: Realization of surface charge measurement with a charge amplifier circuit.

This principle is widely used for amplification of signals from piezoelectric sensors and photo-diodes. The charge amplifier will balance the charge Q(x) injected into the negative input by charging the feedback capacitor C_f . The resistor R_f bleeds the charge off capacitor C_f at a low rate to prevent the amplifier from drifting into saturation. The value of R_f and C_f sets the low cutoff frequency f_{low} of the amplifier

$$f_{\text{low}} = \frac{1}{2\pi C_f R_f}.$$
 (9)

The action of the amplifier maintains 0 V across its input terminals (Karki 2000). Thus the backside electrodes of the samples are virtually connected. The amount of charge O(x) flowing from one material's backside to another is then inversely proportional to the air capacitance and proportional to the combined capacitance of C_{PTFE} and C_{Nylon}

$$Q(x) = C_{\text{(PTFE+Nylon)}} \frac{Q_n}{C_{\text{air}}} = C_{\text{(PTFE+Nylon)}} \frac{Q_n}{\varepsilon_0 \frac{A}{x}}.$$
 (10)

Here $C_{(PTFE+Nylon)}$ is the total capacity of the PTFE and the Nylon sample in series while Q_n is the surface charge after *n* contacts. The ratio between the surface charge and the surface area A can be replaced with the surface charge density σ_n . The output voltage U_a of the charge amplifier is proportional to Q(x) divided by C_f . Equation 10 then becomes

$$U_{\rm a} = -\frac{Q(x)}{C_{\rm f}} = -\frac{C_{\rm (PTFE+Nylon)}}{C_{\rm f}} \frac{\sigma_n}{\varepsilon_0} x. \tag{11}$$

The output voltage U_a is proportional to the surface charge density times displacement. Consequently the charge density can be reverse calculated from these two values. The series capacitance of the samples was experimentally determined and is listed in Table 1.

Experimental Procedure

To analyze the influence of the three main parameters (force, temperature and humidity) and their interactions, each parameter was varied on the three levels referred in Table 2. Each run was replicated three times to reduce the statistical measurement error. This was a total of 81 measurements. For analysis the median values of the three repetitions were calculated. The samples were rinsed in isopropanol and then in DI-water to remove the initial charge before every run. Finally they were dried in air for one hour. Before starting a measurement, the samples were cooled or heated for another 20 minutes inside the temperature chamber so that they were fully acclimated to the chamber temperature and humidity settings. The measurements were recorded over a time period of 1000 s with a sample rate of 100 points/s. The movement speed was set to 2 mm/s and the maximum displacement between the sample surfaces was set to 2 mm. The surface charge density was calculated based on eq. (11). The values after 5, 50 and 150 contacts were used to compare the parameter's influence. Thus the charge increase rate and also the charge saturation was evaluated.

Results

Figure 9 shows typical curves of charge build up with repeated contacts under the three levels of contact force at 25°C and 50% RH. Each value in the figure represents

Table 2: Parameter variation levels.

Level	Contact force variation [N]	Temperature and rel. humidity (RH) [°C at %]
1	200	9 at 60
2	300	25 at 50
3	400	45 at 17

Table 3: Comparison between experimental results and previous studies by Greason (2000), Liu, Oxenham, and Seyam (2013) and Lee et al. (2013).

	Kleyman et al. (2016)	Greason (2000)	Liu, Oxenham, and Seyam (2013)	Lee et al. (2013)		
Increase of	Maximum surface charge density σ					
Force	lin. increasing	-	Increasing	_		
Temperature	lin. decreasing (>spec.RH)	lin. decreasing	No trend	_		
RH	lin. decreasing (>spec. T)	lin. decreasing	No trend	_		
Contact area or decreasing roughness	increasing	_	_	Increasing		
Young's modulus	$rac{\partial \sigma}{\partial F}$ increasing	_	_	_		

the mean of three repetitions. The results indicate that the charge density growth rate is higher at the beginning and slows down after several contacts until saturation is reached. This could be a result of a rising potential difference between the surfaces and a higher discharge rate. According to previous studies (Greason 2000), charge

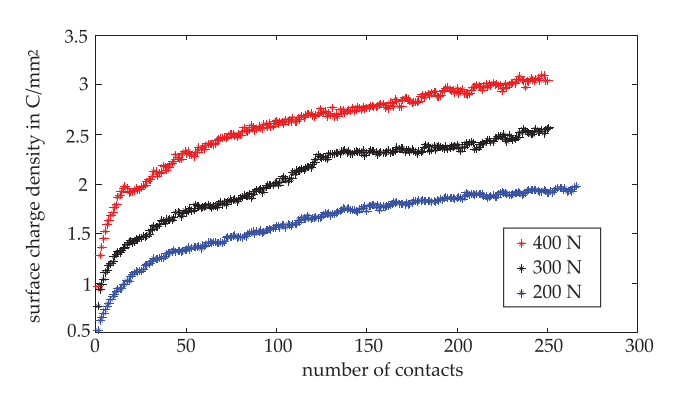


Figure 9: Charge generated between PTFE and Nylon by repeated contact at different contact force (at 25°C and 50% RH).

accumulation and charge leakage are balanced at the point of saturation. Furthermore the data show that the growth rate and also the saturation level are strongly related to the applied contact force. This confirms actual studies (Liu, Oxenham, and Seyam 2013), however at this point it remains unclear if the rising surface charge is resulting from a higher real contact area (Wang 2013) or from higher mechanical stress (Lacks and Sankaran 2011).

Figure 10 shows the surface charge density under variation of contact force, temperature and relative humidity (RH) for the two different sample pairs after a specific number of contacts. It is evident from these results that the sample pair No. 2 in general produces less surface charge. Referring to Figure 6 PTFE sample No. 2 has a much higher surface roughness than the other samples. It can be concluded that the large asperities on PTFE sample No. 2 entail less contact area between the samples. This fact proves the contact area theory of surface charging. This result is reasonable since a correlation between charge density and surface micro-roughness was already

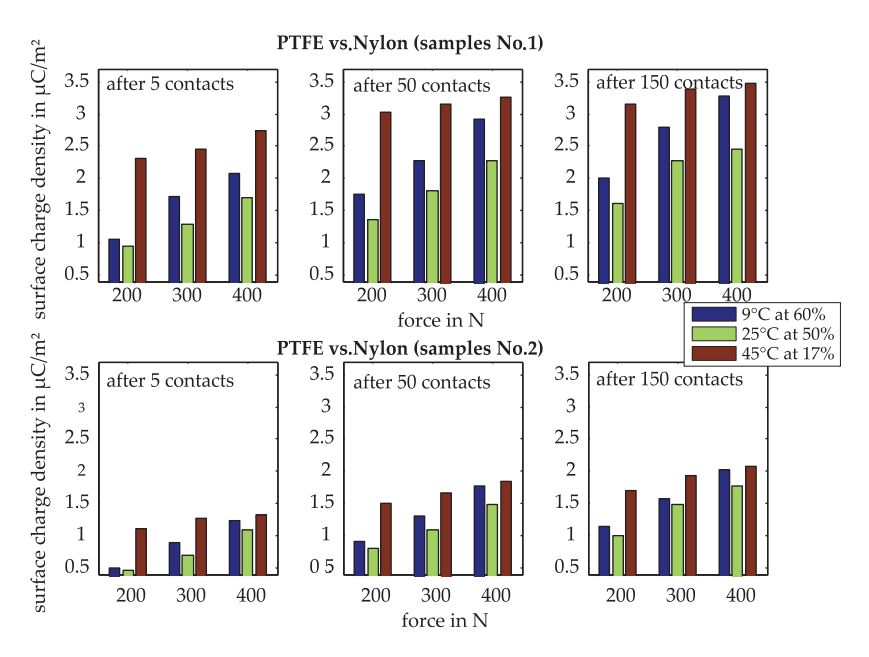


Figure 10: Surface charge density on PTFE vs. Nylon after 5, 50 and 150 contacts under variation of contact force and temperature/RH.

found for polymer versus metal contact (Coste and Pechery 1981). From Figure 10 it is also evident that the surface charge grows linearly with contact force for same settings of temperature and relative humidity. Proof can be found if the peaks of the same colored bars in Figure 10 are connected by lines of best fit. These lines of best fit are replotted in Figure 11. With the findings from Figure 11 we can state that there is a remarkable connection between sample temperature and the impact of contact force on surface charge generation. A higher sample temperature or a lower relative humidity reduces the slope of the line of best fit. This could be the result of a softening of the materials. As Figure 7 shows the Young's modulus of the sample materials changes in the considered temperature range. Assuming small deformations and a constant deformation frequency (which is the case in our study), it can be claimed that a lower Young's modulus results in a higher deformation of surface asperities. The real contact area between materials is defined as the sum of cross-sectional areas formed by asperity contacts (Durig and Stadler 1997). At the same level of contact force a softer material has more real contact area with its contact partner than

a more rigid material with the same roughness characteristics. This is because the asperities are getting more deformed as Figure 12 illustrates. The relative change of contact area at higher temperatures under force variation is less because the contact area is already high. This is an important insight considering previous publications where no specific trend in terms of charge generation of polymeric materials and temperature or relative humidity was found (Liu, Oxenham, and Sevam 2013). At first glance it appears that there is no relation between temperature, humidity and surface charge saturation. This is most likely because the rising temperature correlates with a relative humidity drop. As published in a previous work by (Greason 2000) there is a linear relationship between the triboelectric charge saturation values and temperature or relative humidity for metal versus polymer contact. In their study the saturation values are decreasing with a higher temperature (at constant RH) and also with higher relative humidity (at constant temperatures). These two factors are counteracting each other in our experiments, but since a linear relationship was already reported for metal versus polymer contact this is reason enough to

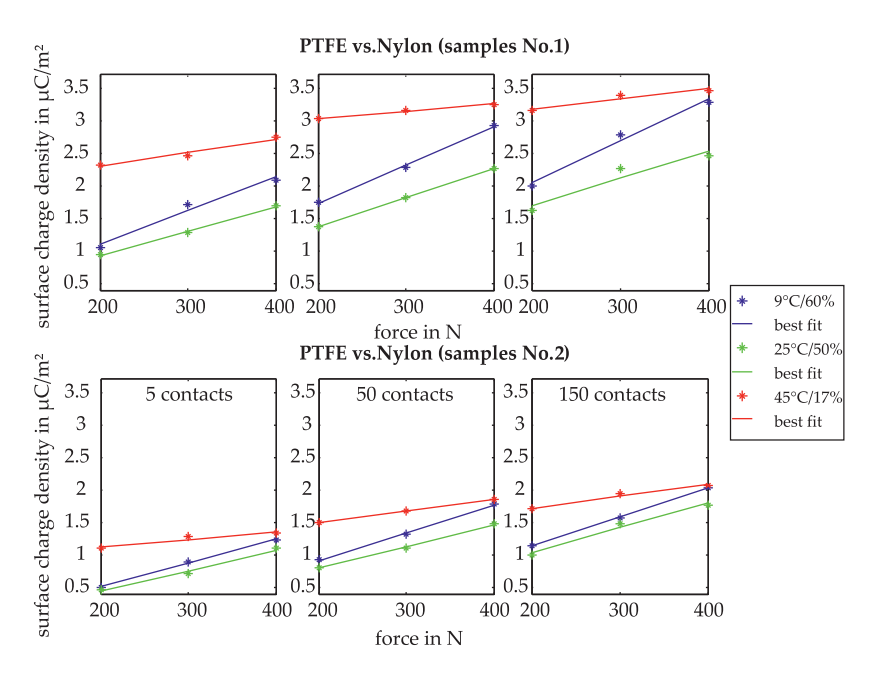


Figure 11: Line of best fit for surface charge density on PTFE vs. Nylon after 5, 50 and 150 contacts.

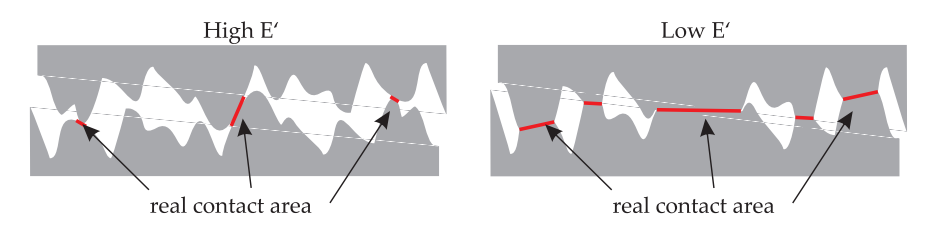


Figure 12: Illustration of the real contact area for a rigid (high E') and a soft (Low E') material.

assume linear dependencies for a polymer versus polymer contact as well. Based on this hypothesis a linear model from the three parameters (force, temperature and relative humidity) is formulated

$$\sigma = \alpha_0 + \alpha_1 T + \alpha_2 RH + \alpha_3 F + \alpha_4 T \cdot F + \alpha_5 RH \cdot F + \alpha_6 T \cdot RH + \alpha_7 T \cdot RH \cdot F.$$
 (12)

Here σ is the surface charge density, T is the temperature in °C, RH is the relative humidity in percent and the vector α contains the model parameter. It can be seen that there are 8 model parameter that must be determined. The same number of linearly independent equations is necessary to solve this equation. There are 9 data sets for each pair of samples considering the measurement data after 150 contacts (which is almost saturation). We have used 6, 7 and 8 of our data sets to approximate the model parameter by a numerical least squares approach and compared the results in Figure 13. As it can be seen in this figure there is almost no deviation between the estimated model parameter for different numbers of equations. Since the remaining data sets are not incorporated in the calculation they can serve as additional data points for model validation. Therefore the parameters are determined for both pairs of samples with just 6 equations and the accuracy of the approximation is controlled. The theoretical surface charge is recalculated according to eq. (12) with the experimental settings (temperature, humidity, force) from the determined model parameter α . Figure 14 shows the comparison between the measurement data and calculated values. The remaining 3 control values which were not used for model parameter calculation are highlighted in red. The calculation shows an average relative error of 1.9% and a maximum deviation of 10% which is a very satisfying result. After the model parameter are identified eq. (12) is used to investigate the isolated influence of each single external factor (T, RH and F) in the space of the experimental setup limits. Figure 15 shows a calculation of the surface charge

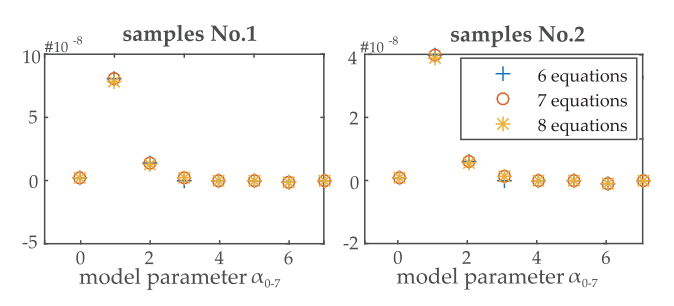


Figure 13: Comparison between approximated model parameter using 6, 7 and 8 equations.

density of sample pair No. 1 at a contact force of 400 N for different settings of temperature and relative humidity. It is evident that the charge density is decreasing with rising temperature and is increasing with falling relative humidity as already reported for polymer versus metal contact. In particular, the interaction of different temperature and humidity settings is interesting as there can be found a characteristic point. A previous publication by (Greason 2000) stated that for polymer versus metal contact the slope of the charge versus temperature characteristic decreases as the relative humidity increases. Another study says that there is no specific trend of the charge generated in terms of temperature and humidity found for polymer versus polymer contact (Liu, Oxenham, and Seyam 2013). As Figure 16 shows, this is different for the PTFE versus Nylon contact in the present paper. Here, the slope of the charge versus temperature characteristic increases as the relative humidity increases. This fact suggests that air humidity plays a different role in polymer versus polymer triboelectric charging than in polymer versus metal charging. There is also a characteristic temperature point where relative humidity does not affect triboelectric charging at all. This is the point where all the lines in Figure 16 intersect each other. It is evident that this intersection point is located at different temperatures for the two pairs of samples. Since the same material was used for both pairs with exactly the same elastic properties, the difference can not be related to the Young's modulus change. This difference must be originated from the surface structure of the materials. This result shows that the micro-roughness is affecting the triboelectric charging in two ways: (i) reduction of the real contact area between contact partners and therefore a lower triboelectric charge saturation, (ii) change of the temperature and humidity versus charge characteristics.

Conclusion

A series of experiments were performed to gain a better understanding of the triboelectric charging of polymeric materials after repeated contact. PTFE and Nylon were chosen as sample materials for this study since they are classified on opposite sides of the triboelectric series. The impact of surface roughness, contact force, temperature and relative humidity on triboelectric charging was investigated by varying these factors on different levels, see Tables 1 and 2. The results are summarized in Table 3. It was shown that roughness is an essential factor in triboelectric charge generation. The sample

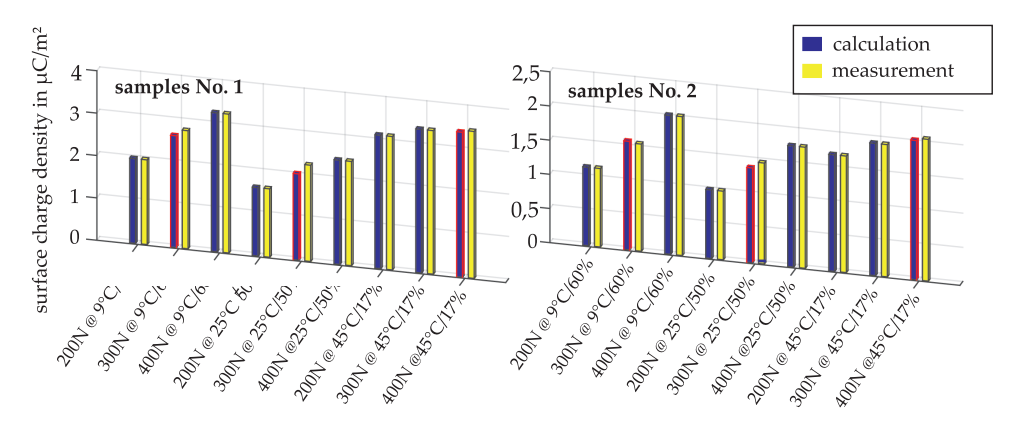


Figure 14: Comparison between actual measurement data and a calculation using the determined model parameter. The values which are highlighted in red were not used for parameter estimation.

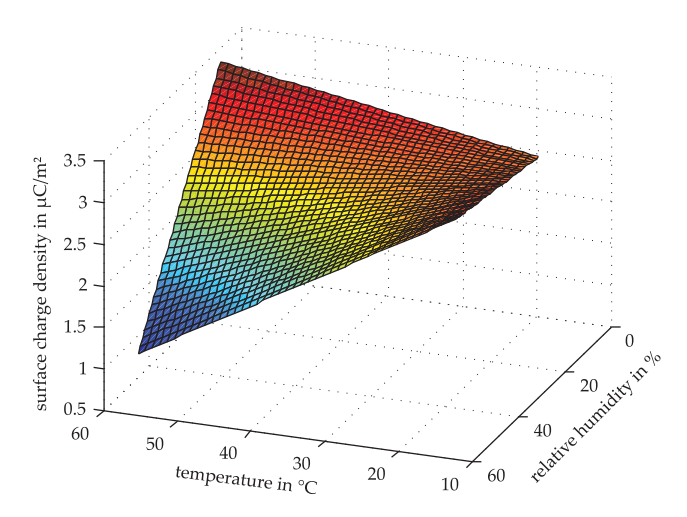


Figure 15: Triboelectric charge saturation for PTFE/Nylon contact as a function of temperature and relative humidity. Determined from model parameter (sample No. 1).

with bigger asperities and thus less contact area produced a significantly smaller surface charge compared to the more planar sample. Further it was proved that triboelectric charge increases linearly with increasing contact force. The gradient of the increase is related to the elastic

modulus of the materials. The study also demonstrates that the impact of temperature and relative humidity on charge saturation within the experimental limits is linear. Based on these findings a mathematical formulation was given, which allows the quantitative determination of surface charge in dependence to the three above-stated parameters. This formulation enables an a priori estimation of the surface charge for different operating points of a triboelectric energy harvester after a few preliminary experiments, which serve to determine the model parameter vector. Furthermore, an equation was given for the power output of a triboelectric energy harvester in a quasi static regime, which contains geometrical and mechanical parameters of the device. With these two base equations, one can design and optimize triboelectric energy harvesters so that they are perfectly adapted to environmental conditions and excitation forces. Finally, a screening of the temperature versus charge behavior at the theoretical level was performed. It shows that the roughness is effecting not only the surface charge saturation value but the fundamental charging characteristic. There exist a temperature point where lines of different relative humidity intersect and thus do not control surface

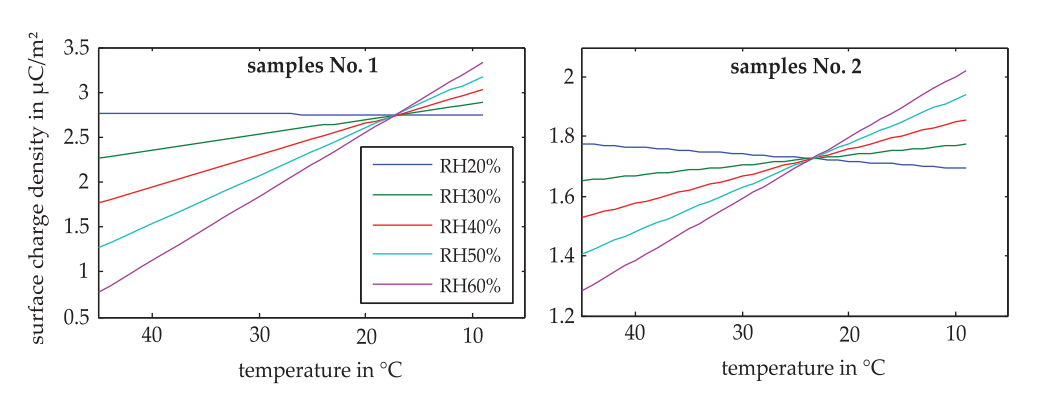


Figure 16: Charge saturation values of PTFE/Nylon contact for different settings of temperature and relative humidity.

charge saturation, which must be a function of the surface roughness. This observation is based on an interpolation of the measuring data inside the measurement range. As there is no experimental proof for this fact yet, this hypothesis should be proved also on an experimental level in future publications. Still, this and the fact that the Young's modulus is affecting triboelectric charging of polymers is a novel insight in triboelectric research. Along with the mathematical formulation this offers new methods of designing better triboelectric energy harvesting systems.

References

- Bhushan, B. 2000. Modern Tribology Handbook, Two Volume Set. Florida: CRC Press.
- Boisseau, S., G. Despesse, and B. A. Seddik. 2012. "Electrostatic Conversion for Vibration Energy Harvesting." In Small-Scale Energy Harvesting, edited by D. M. Lallart. Rijeka: InTech.
- Bright, A. W., and B. Makin. 1969. "Modern Electrostatic Generators." Contemporary Physics 10: 331-353, http://dx.doi.org/10.1080/00107516908204792.
- Calleja, G., A. Jourdan, B. Ameduri, and J.-P. Habas. 2013. "Where Is the Glass Transition Temperature of Poly(tetrafluoroethylene)? A New Approach by Dynamic Rheometry and Mechanical Tests." European Polymer Journal 49: 2214-2222. https://hal.archives-ouvertes.fr/hal-00844535.
- Chun, J., J. W. Kim, W.-s. Jung, C.-Y. Kang, S.-W. Kim, Z. L. Wang, and J. M. Baik. 2015. "Mesoporous Pores Impregnated with au Nanoparticles as Effective Dielectrics for Enhancing Triboelectric Nanogenerator Performance in Harsh Environments." Energy & Environmental Science 8: 3006-3012. http://dx.doi.org/10.1039/C5EE01705J.
- Coste, J., and P. Pechery. 1981. "Influence of Surface Profile in Polymer-metal Contact Charging." Journal of Electrostatics 10: 129-136. http://www.sciencedirect.com/science/article/pii/ 0304388681900322.
- Durig, U., and A. Stadler. 1997. Micro/Nanotribology and Its Applications. Springer Science+Business Media, chapter Adhesion on the Nanometer Scale.
- Evstatiev, M. 1997. Handbook of Thermoplastics. Marcel Dekker, chapter Polyamides.
- Galembeck, F., T. A. L. Burgo, L. B. S. Balestrin, R. F. Gouveia, C. A. Silva, and A. Galembeck. 2014. "Friction, Tribochemistry and Triboelectricity: Recent Progress and Perspectives." RSC Advances 4: 64280-64298. http://dx.doi.org/10.1039/ C4RA09604E.
- Greason, W. D. 2000. "Investigation of a Test Methodology for Triboelectrification." Journal of Electrostatics 49: 245-256. http://www.sciencedirect.com/science/article/pii/ 50304388600000139.
- Ha, M., J. Park, Y. Lee, and H. Ko. 2015. "Triboelectric Generators and Sensors for Self-powered Wearable Electronics." ACS Nano 9: 3421-3427. http://dx.doi.org/10.1021/acsnano.5b01478, pMID: 25790302.

- Karki, J. 2000. "Signal Conditioning Piezoelectric Sensors." Technical report, Texas Instruments, application Report SLOA033A.
- Kim, H., Y. Tadesse, and S. Priya. 2009. Energy Harvesting Technologies. Springer, chapter Chapter 1 – Piezoelectric Energy Harvesting.
- Lacks, D. J., and R. M. Sankaran. 2011. "Contact Electrification of Insulating Materials." Journal of Physics D: Applied Physics 44: 453001. http://stacks.iop.org/0022-3727/44/i=45/a=
- Lee, S., Y. Lee, D. Kim, Y. Yang, L. Lin, Z.-H. Lin, W. Hwang, and Z. L. Wang. 2013. "Triboelectric Nanogenerator for Harvesting Pendulum Oscillation Energy." Nano Energy 2: 1113-1120. http://www.sciencedirect.com/science/article/ pii/S221128551300147X.
- Liu, L., W. Oxenham, and A.-F. M. Seyam. 2013. "Contact Electrification of Polymeric Surfaces." Indian Journal of Fibre & Textile Research 38: 265-269.
- Meirovitch, L. 1970. Methods of Analytical Dynamics. New York, NY: McGraw-Hill Book Company.
- Niu, S., S. Wang, L. Lin, Y. Liu, Y. S. Zhou, Y. Hu, and Z. L. Wang. 2013. "Theoretical Study of Contact-mode Triboelectric Nanogenerators as an Effective Power Source." Energy & Environmental Science 6: 3576-3583. http://dx.doi.org/10.1039/C3EE42571A.
- Niu, S., and Z. L. Wang. 2015. "Theoretical Systems of Triboelectric Nanogenerators." Nano Energy 14: 161-192. http://www.sciencedirect.com/science/article/pii/ S2211285514002353, special issue on the 2nd International Conference on Nanogenerators and Piezotronics (NGPT 2014).
- Peacock, C. A., and J. Andrew. 2006. Polymer Chemistry -Properties and Applications. Munich: Hanser Publishers.
- Rae, P. J., and D. M. Dattelbaum 2004. "The Properties of Poly(tetrafluoroethylene) (ptfe) in Compression." Polymer 45: 7615-7625.
- Roundy, S., P. K. Wright, and J. M. Rabaey. 2004. Energy Scavenging for Wireless Sensor Networks. Springer Science+Business Media, chapter Electrostatic Converter Design.
- Shaw, P. E. 1917. "Experiments on Tribo-electricity. i. the Tribo-electric Series." Proceedings of the Royal Society of London A: Mathematical, Physical and Engineering Sciences
- Tang, W., C. Zhang, C. B. Han, and Z. L. Wang. 2014. "Enhancing Output Power of Cylindrical Triboelectric Nanogenerators by Segmentation Design and Multilayer Integration." Advanced Functional Materials 24: 6684-6690. http://dx.doi.org/10.1002/adfm.201401936.
- Wang, Z. L. 2013. "Triboelectric Nanogenerators as New Energy Technology for Self-powered Systems and as Active Mechanical and Chemical Sensors." ACS Nano 7: 9533-9557. http://dx.doi.org/10.1021/nn404614z, pMID: 24079963.
- Wang, Z. L. 2014. "Triboelectric Nanogenerators as New Energy Technology and Self-powered Sensors - Principles, Problems and Perspectives." Faraday Discussion 176: 447-458. http://dx.doi.org/10.1039/C4FD00159A.
- Zhu, G., J. Chen, T. Zhang, Q. Jing, and Z. L. Wang. 2014. "Radial-arrayed Rotary Electrification for High Performance Triboelectric Generator." Nat Commun 5. http://dx.doi.org/10.1038/ncomms4426, article.